Aerodynamic's measurements of wing's parameters

Adrián Grande, Sofía Martínez, Ignasi Piqué, Jordi Tononi and Francisco Tugores
Physics Engineering, Universitat Politècnica de Catalunya,
Campus Nord UPC, 08034-Barcelona, Catalunya
(Aerospace Engineering Dvision, Physics Department, Campus del Baix Llobregat, 08860-Castelldefels, Catalunya)
(Dated: May 27, 2017)

The interaction between fluids and bodies is a complex phenomenon which is behind the forces observed in flight. Here we analyze the main aerodynamics forces, lift and drag, in several wing profiles and a cylinder. We consider the two main parameters of study, the drag and lift coefficients. These parameters were measured by using a wind tunnel for different wing profiles, at different angles of attack, and for a cylinder. The effect of winglets was also studied. The study allowed us to understand the elemental behavior of wings in planes and the reason to include winglets to improve the aerodynamic efficiency.

Nowadays traveling by plane is the fastest and safest way to travel. However, it's hard to believe how a plane which weights around 300.000 kg is able to fly long distances at high velocities. The goal of this project is to understand the physical principles that explain the behavior of the main component of an airplane: the wing. Several experiments were performed in a windtunnel. Aerodynamic forces on different wing profiles and a cylinder were measured in order to determinate the aerodynamic parameters of the bodies: the Drag coefficient and the Lift coefficient. The experiments showed how this parameters vary with the geometry of the wing profile and the angle of attack. The first set of measurements were performed on a symmetric wing profile. Then, we designed and constructed two asymmetric wings with the same profile, with and witut winglets, to see the difference of their behavior and characteristics in the windtunnel. Measures on a cylindrical body were taken to determinate the Drag coefficient with different techniques. The performed measurements allowed us to observe some fundamental phenomena that take place in the wing of an airplane, such as the lost of lift and the detachment of the boundary layer.

Dynamic pressure, Reynolds and Mach numbers and dynamic similarity are basic concepts in aerodynamic measurements. When a fluid hits a body one can measure the pressure in the flow direction and in a direction normal to the flow. These are the total (P_t) and static pressure (P_s) respectively. The difference between them is the dynamic pressure, P_d, defined as:

$$P_t - P_s = P_d = \frac{\rho v^2}{2} \tag{1}$$

where ρ is the density of air and v is the speed of the flow relative to the object. The Reynolds number is a dimensionless coefficient defined as:

$$Re = \frac{v_s D}{\nu} \tag{2}$$

where v_s is the upstream velocity or the fluid, D is the characteristic length of the body and ν is the kinetic viscosity of the fluid. The Reynolds number expresses the ratio of inertial (resistant to change or motion) forces to viscous (heavy and gluey) forces and is used to predict the fluid flow regime. Laminar flow occurs at low Reynolds numbers, where viscous forces are dominant, and is characterized by smooth, constant fluid motion and turbulent flow occurs at high Reynolds numbers and is dominated by inertial forces, which tend to produce chaotic eddies, vortices and other flow instabilities. The Mach number gives the ratio of the speed of the aircraft to the speed of sound. It is defined as:

$$M = \frac{v}{u} \tag{3}$$

Where v is the velocity and u is the sound velocity.The Mach number is primarily used to determine the approximation with which a flow can be treated as an incompressible flow. This number defines some regimes but we are just interested in subsonic regime with $M < 1$. Finally two different flows are dynamically similar if the bodies and any other solid boundaries are geometrically similar for both flows and the similarity parameters, the Reynolds and Match. Therefore, in a limited sense, we can say that flows over geometrically similar bodies at the same Mach and Reynolds numbers are dynamically similar, and hence the lift, drag, and moment coefficients will be identical for the bodies. If a scale model of a flight vehicle is tested in a wind tunnel, the measured lift, drag, and moment coefficients will be the same as for free flight as long as the Mach and Reynolds numbers of the windtunnel test-section flow are the same as for the free-flight case. This requirement is almost impossible to fulfill in scale-model measurements, but as wing profiles in planes work always at high Re, where the flow is turbulent, it is essential to ensure that Re_{sc} in the scale model be high enough to be in the turbulent regime. In practice, it is enough to ensure that $Re_{sc} > 10000$.

The basic parameters of a wing, namely the lift (C_L) and drag (C_D) coefficients are related to the wing's geometry. These aerodynamic coefficients are defined by

$$C_d = \frac{f_d}{\frac{1}{2}\rho S v^2}, \quad C_l = \frac{f_l}{\frac{1}{2}\rho S v^2} \tag{4}$$

where f_d andf_l are respectively the drag and lift forces.

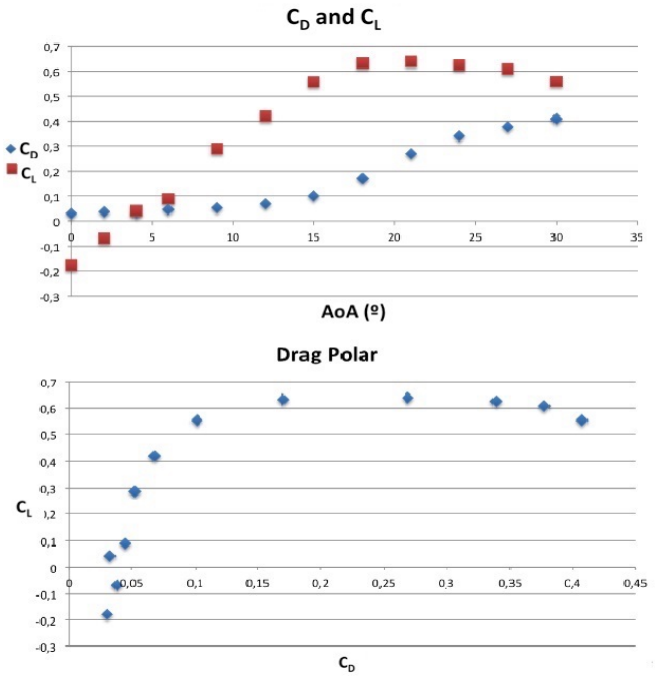

FIG. 1. Top: Drag (C_D) and lift (C_L) coefficients as a function of the angle of attack AoA. Bottom: Drag polar plot displaying C_L vs. C_D.

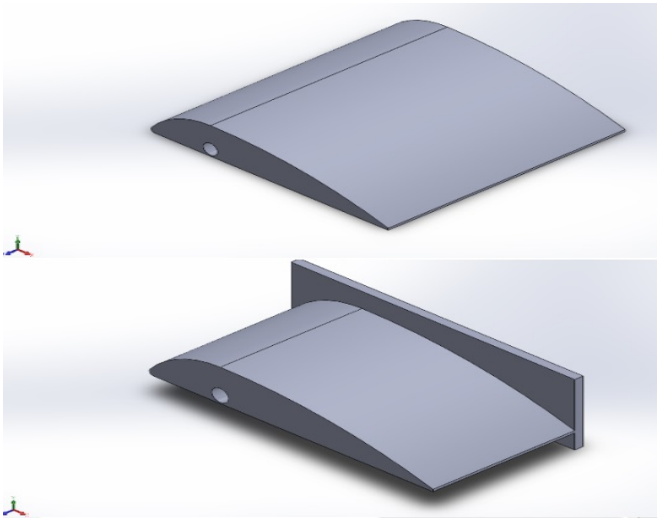

FIG. 2. Final design of the two wings. The second one represents one half of the entire wing, as both halves were 3D printed separately. All the wing parameters have the same value, they only differ in the winglets or not presence.

In order to understand the basic aerodynamic properties of aircrafts' wings we designed an experiment to measure the aerodynamic coefficients in a symmetric profile as a function of the angle of attack. In this first experiment a symmetrical profile is studied. Placing the wing inside a wind tunnel, the coefficients are obtained as a function of the angle of attack (AoA) by measuring the lift and drag forces and the P_d and P_t with a Pitot tube. The velocity of the air was calculated from eqn. (3), allowing to obtain the values of both coefficients. For every AoA, the aerodynamic forces were measured for different air velocities and the value of the aerodynamic coefficients was obtained by linear regression.

Figure 1 shows that symmetric wing's resistance increases with the angle of attack. The ratio $\frac{C_L}{C_D}$ has a maximum value when AoA $\sim 12°$. For angles of attack greater than $20°$ the C_L coefficient starts to decrease and the wing stalls. The value of C_L for a symmetric profile is expected to be null at AoA$= 0°$. The observed value is attributed to the fact that the wing was not positioned perfectly parallel to the air flow at AoA$= 0°$.

The pressures' difference between the bottom (intrados) and the top (extrados) of a wing is the main responsible of the structure's lift, but also the main cause of the vortex generated. In the wing tip there is nothing avoiding the air flowing to lower pressures. Furthermore, the wing has already passed a point when the air moves, due to the high velocity of the structure. This phenomenon generates whirlwinds, which cause turbulences. With the objective of minimizing this problem, wind tip devices, also called winglets, are usually installed in planes. This device avoids the direct connection between the intrados and the extrados, so the drag force is reduced and wind tip lift is increased. Moreover, the fuel consumption is decreased. These devices were the aim of the following experiment. The design of two asymmetric wing profiles was performed using the mechanical modelling software Solid Works - see Figure 2. The goal of this experiment was to compare the drag and lift aerodynamic parameters of the wing profile with and without winglets from the wind tunnel's measurements.

The results confirmed previous statements (Figure 3). The increase of the lift force in the winglet profile in front of the original is obvious. However, the winglet profile gets stalled at a lower angle of attack, probably due to the lack of aerodynamics in the winglets' design. Concerning this topic, the stall point is not a well-defined point in these measures, due to the transverse section of the tunnel. According to the literature[4], when the front surface of the object under test is larger than 10% of the tunnel cross-section a blocking effect appears which makes the fluid to interact both with the object and the tunnel walls simultaneously. This blocking effect may avoid the normal behavior of the flow around the profile during stall.

Next we measured the drag force on a cylinder inside air at a speed of 10 m/s by several methods and compare the results obtained. The direct measurement of the drag force on the three component scale gave a value of $1.8N$. The two alternative measurements were performed by measuring the air velocity profile in the wake of the cylinder and by measuring the pressure distribution on the cylinder surface.

The physical basis of the first experiment on the cylin-

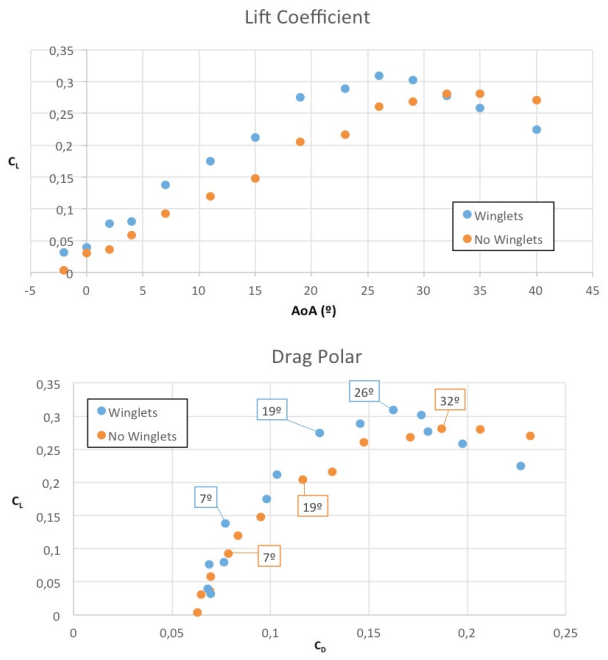

FIG. 3. Lift and drag measurement of the wing profiles with and without winglets. Top: Lift coefficient vs. AoA. Bottom: lift vs. drag coefficients - Drag polar plot - showing some AoA values.

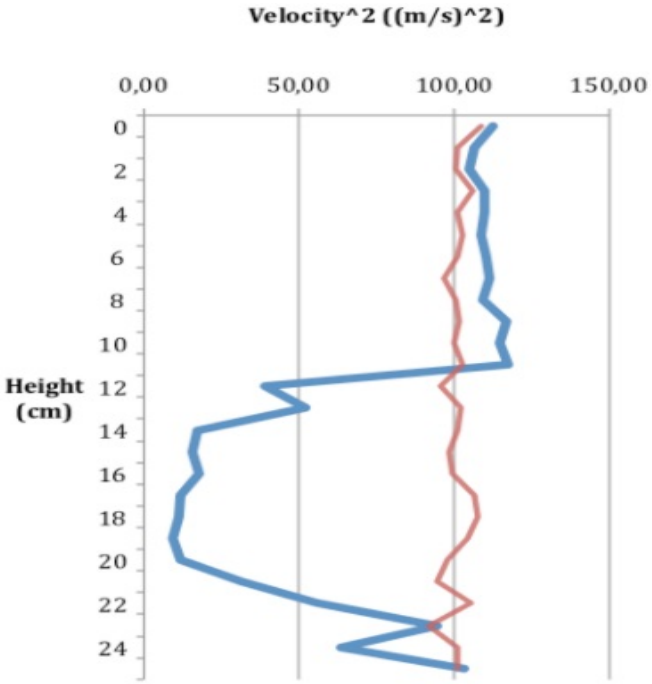

FIG. 4. Upstream - red - and downstream - blue - squared air velocity vs height measured by two hot wire anemeters, of the two hot wires. The difference area between them times the length of the cylinder and the air density gives directly the drag force.

der is the impulse theorem applied to the flow:

$$\vec{F}\Delta t = \Delta\vec{p}, \quad \vec{F} = \frac{d\vec{p}}{dt} \tag{5}$$

where $\vec{p}$ is the momentum carried by the flow and $\vec{F}$ is the force acting on the flow; in this case, the reaction force due to the cylinder. To apply this theorem a control volume of fluid containing the object being tested must be considered. The control volume is taken as a parallelepiped with its x axis aligned to the flow. The height h of the control volume must be enough to include the wake of the cylinder, and the width w will be that of the cylinder. The mass flow of a fluid across a surface $S = hw$ normal to the flow is $\dot{m} = \rho S\vec{v}$, where ρ is the density of the fluid. The upstream flow entering the volume carries a momentum $\vec{p}_{in} = \dot{m}_{in}\vec{v}_{in}$. Analogously, the downstream flow carries $\vec{p}_{out} = \dot{m}_{out}\vec{v}_{out}$. The time derivative of the momentum can be approximated by its space derivative inside of the considered volume. Neglecting the flow through the surfaces parallel to the flow, the change in the momentum is given by:

$$\frac{\partial\vec{p}}{\partial t} \sim \frac{\partial\vec{p}}{\partial x} = \dot{p}_{out} - \dot{p}_{in} = \dot{m}_{out}\vec{v}_{out} - \dot{m}_{in}\vec{v}_{in} = \vec{F} \tag{6}$$

The cylindrical profile was placed inside the windtunnel and the velocity of the wind was measured using two hot wire anemometers. One of the anemometers was moved vertically - z direction -, inside the windtunnel and just behind the center of the cylinder, from the roof to the floor with intervals of 1 cm. The other was fixed, simulating the wind velocity without the cylindrical profile. This second hot-wire anemometer shows a quite constant profile of velocities, while the first anemometer shows variations in the velocities do to the turbulence generated by the cylinder. The flow speed in the wake was taken as constant in the cylinder axis - y - direction, and equal to that measured in the center of the cylinder. Then, the flow of momentum was computed by

$$\dot{p}_{in,out} = \int_0^h \rho w v_{in,out}^2 dz \tag{7}$$

and the integral was computed numerically by the 3/8 composed Simpson method.

Figure 4 shows the upstream and downstream velocity profiles. The reduction of the downstream velocity, due to the cylinder obstruction, is clearly seen. Application of eqn (6) gives a Drag force of $2.6 \pm 0.2N$ with a confidence interval of 97.5%, while the force measured by the scale was $1.8N$. That is, the indirect measurement overestimates the cylinder drag. This is most probably due to the two approximations performed, namely that the speed is the same along the cylinder axis and that the flow in the upper and lower surfaces is parallel to the initial stream.

The goal of the second experiment was to measure of the pressures through the surface of the same cylinder.

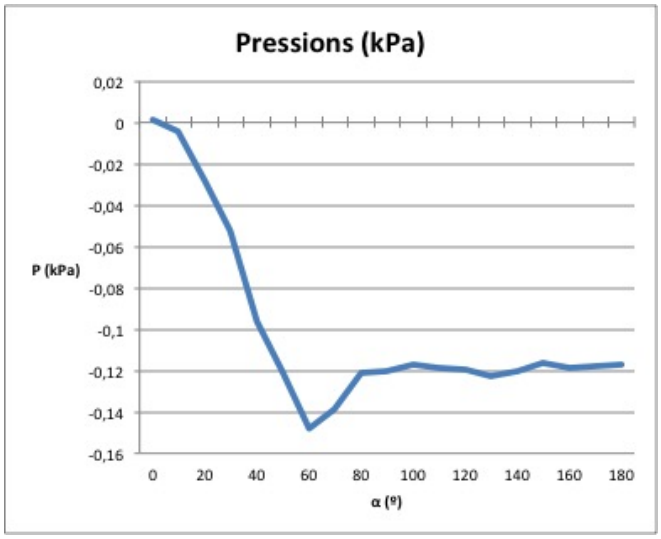

FIG. 5. Profile of pressions among the surface of the cylinder in function of its angle related to the wind direction.

The symmetry of the object allows us assume the generalization that the measure performed in the center of the object is the same along all the length of its section and it's the same on the upper and lower part of the cylinder. This corresponds to the infinite length approximation and neglects the side effects at the end of the cylinder.

The pressure measurements were performed at increments of 10º between 0º and 180º. Each pressure P_i is related to the force dF_i acting in the approximated rectangular section dS of 10º on the surface of the cylinder by $P(\alpha_i) = dF_i/dS$, and $dS = L\pi r/18$ except for the initial and final measurement where $dS_{0,18} = L\pi r/36$. The drag force is the addition of the corresponding force components in the horizontal axis, namely $dF_{D,i} = P(\alpha_i)\cos(\alpha_i)dS$. Furthermore, the pressure used was the static pressure which corresponds to $P_{static} = P_{measured} - P(90º)$. Where $P(90º)$ is the pressure measured perpendicularly to the wind direction. Finally, the sum of all forces is the Drag Force, giving $F_d = 0.97 \pm 0.16N$ with a confidence interval of 97.5%. It is worth to note that now the measured drag is lower than that measured directly on the three-component scale. The reason for this underestimation is the assumption of infinite cylinder length. It is well known in the literature that side effects induce additional drag which are be considered in this measurement.

Summarizing, aerodynamic measurements on several bodies were performed in a windtunnel. Measurements on a symmetric wing profile allowed to compute its aerodynamic coefficients at different angles of attack. The drag polar was computed, and the best aerodynamic performance was found at an angle of attack of 12º. Next a non-symmetric profile was tested with and without winglets, allowing to observe the increase in the lift coefficient when winglets are used. Finally, the drag coefficient of a cylinder was determined directly, by using a three component scale, determining the loss of momentum of the flow and measuring the pressure distribution on the cylinder surface. It was found that the loss of momentum method overestimates the cylinder drag while the pressure distribution method underestimates it. The reasons for these differences were also discussed.

I. MATERIALS & METHODS

Force measurements were performed on a TQ three-component scale, which allows to determine the lift, drag and pitch on a body. Pressure data was determined with a TQ array of pressure gauges, equipped also with a Pitot tube which allowed us to measure the free stream velocity. Both force and pressure sensors were connected to a personal computer through a TQ communication device. Hot wire anemometry was performed by using a Dantec mini-CTA measurement system. Data was processed using Excel and statistical means and deviations were computed.

The first experiment was performed on a symmetrical wing of 30 cm x 15 cm surface. The second experiment was performed on two asymmetric winds of surface 10 cm x 10 cm and a width of 15 mm; the second of those profiles was supplemented with Winglets of 10 x 10 cm (see fig 2). These wings were designed by Solidworks and printed on a 3D printer. The last experiment was performed on a cylinder of length 30 cm and radius 3 cm.

ACKNOWLEDGEMENTS

We thank Escola d'Enginyeria de Telecomunicació i Aeroespacial de Castelldefels for the experimental support and, particularly, for allowing us the use of their 3D printer.

REFERENCES

[1] Anderson J. D., (1984). Fundamentals of aerodynamics. United States of America. McGraw-Hill, Inc.

[2] How Things Work: Winglets. Air & Space Magazine. September 1, 2001.

[3] Charles G. Lomas, (1986). Fundamentals of Hot Wire Anemometry. Cambridge University Press.

[4] Jewel B. Barlow, William H. Rae, Alan Pope, Low-Speed Wind Tunnel Testing, 3rd Ed., Wiley, 1999